EUROPHYSICS LETTERS 1 October 1998

Europhys. Lett., **44** (1), pp. 31-36 (1998)

Experimental realization of coherent dark-state magnetometers

A. Nagel, L. Graf, A. Naumov(*), E. Mariotti(**), V. Biancalana(**)
D. Meschede and R. Wynands

Institut für Angewandte Physik, Universität Bonn
Wegelerstraße 8, 53115 Bonn, Germany

(received 3 April 1998; accepted in final form 28 July 1998)

PACS. 42.50Gy – Effects of atomic coherence on propagation, absorption, and amplification of light.
PACS. 32.70Jz – Line shapes, widths, and shifts.
PACS. 07.55Ge – Magnetometers for magnetic field measurements.

Abstract. – Coherent population trapping resonances in cesium vapor can be used to determine DC flux densities in the range from 1 μT to 1 mT with typically $3{\cdot}10^{-5}$ relative uncertainty. For fields modulated at a few kHz, we find sensitivities of below 10 pT within 0.5 s integration time. From the signal-to-noise ratio the sensitivity can be extrapolated to $500\,\mathrm{fT}/\sqrt{\mathrm{Hz}}$. A quantitative understanding of the lineshape allows to detect DC fields of several nT even when the Zeeman components of the resonance are not resolved.

The sensitive detection of magnetic fields is of great importance in various fields of science and applications, and many different detectors have been developed. Biomedical applications are currently the domain of SQUID detectors [1], whereas in geophysics and archaeology optical pumping magnetometers [2-4] are frequently used. Sensitivities as high as a few $\mathrm{fT}/\sqrt{\mathrm{Hz}}$ can be reached with SQUID detectors (see, *e.g.*, [5]) which however require cryogenic cooling. For several optical pumping magnetometers sensitivities as low as a few hundred fT have been demonstrated [3, 4, 6] with the current record at $1.8\,\mathrm{fT}/\sqrt{\mathrm{Hz}}$ [7].

A general feature of optical pumping magnetometers is that while higher light intensities give a better signal-to-noise ratio, they also lead to power broadening of the resonance line which eventually degrades sensitivity. A few years ago it was predicted [8, 9] that coherent population trapping resonances [10, 11] could provide superior sensitivity as magnetometers because much higher laser power could be used before the performance would be degraded by power broadening [9]. For typical experimental parameters sensitivities of $10^{-16}\,\mathrm{T}$ for 1 s averaging time were predicted [8]. Apart from these theoretical considerations a magnetometer based on coherent population trapping presents an all-optical device with well-known advan-

(*) Permanent address: Lomonosov University, Moscow, Russia.
(**) Permanent address: Università di Siena, Siena, Italy.

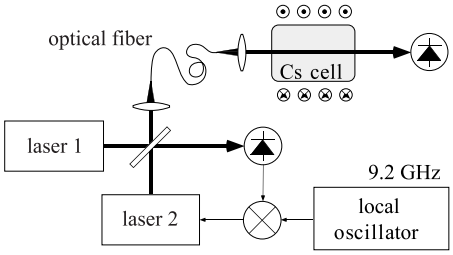

Fig. 1. – Experimental setup for the observation of narrow coherent population trapping resonances in magnetic fields. For clarity only one of the coils around the cell is shown.

tages. For example, the only connections that are needed for the sensor head are two optical fibers leading to the light source and the detector so that no stray magnetic fields are generated near the detector itself (by electrical wires, for instance). Furthermore, in principle a spatial resolution in the μm regime is possible as opposed to typically cm-sized microwave interaction regions.

Coherent population trapping can occur in a so-called Λ-system, where two ground states are coupled to a common excited state via two laser fields near resonantly interacting with one of the transitions each. When the laser difference frequency matches the ground-state splitting the atoms are optically pumped into a coherent superposition of the ground states which no longer absorbs the light. The linewidth of this population trapping resonance is mainly determined by the ground-state relaxation rate. If —as in the case of cesium vapor discussed here— the two lower states are part of the same hyperfine multiplet, electric-dipole transitions between them are forbidden so that radiative damping is negligible. Thus strict control of experimental parameters such as laser difference frequency stability, time-of-flight and collisional broadening results in very narrow experimental linewidths. Recently we have achieved full linewidths below 50 Hz in a cesium vapor cell when neon is used as a buffer gas in order to increase the atomic interaction time [12]. Here we report on our first experiments towards high-sensitivity coherent dark-state magnetometers.

The experimental setup is sketched in fig. 1 [12]. Two laser beams from extended cavity diode lasers resonant with the cesium D_2 transition at 852 nm wavelength are sent through the same single-mode fiber to a cesium vapor cell at room temperature (length 1.8 cm, diameter 2 cm) which in some experiments also contains a few mbars of neon- or silane-coated cell walls. The cesium density is about $3.6 \cdot 10^{10}\,\mathrm{cm}^{-3}$, so the vapor is optically thin as opposed to the theoretical proposals [8, 9]. Typical laser intensities of $1.1\,\mathrm{mW/cm}^2$ were used in a 0.7 cm diameter beam. The second output beam from the beam splitter is needed to electronically control the optical phase of laser 2 via a phase-locked loop [13]. This gives precise control over the laser difference frequency which can be stepped across the resonance by detuning the local oscillator frequency. The intensity transmitted through the cell is detected on a photodiode. Optionally low-frequency modulation of the local oscillator frequency allows to use frequency modulation spectroscopy [14] where the transmitted signal is demodulated by a digital dual-phase lock-in amplifier. For measurements performed without μ-metal shielding, static magnetic fields can be compensated with the help of three mutually perpendicular pairs of coils.

In an external magnetic field the $F = 3$ and $F = 4$ ground states split into 7 and 9 Zeeman levels with energies given by the Breit-Rabi formula. First experiments that resolved Zeeman components of the dark resonance were performed by Akulshin *et al.* [15], Fulton *et al.* [16], and

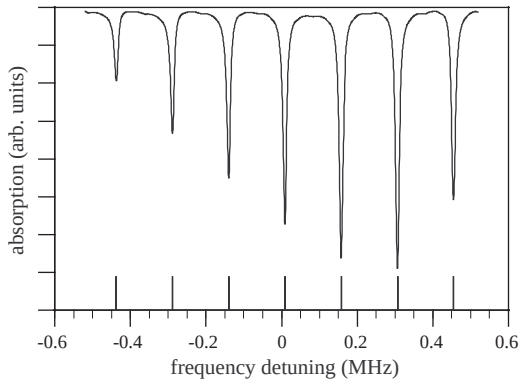

Fig. 2

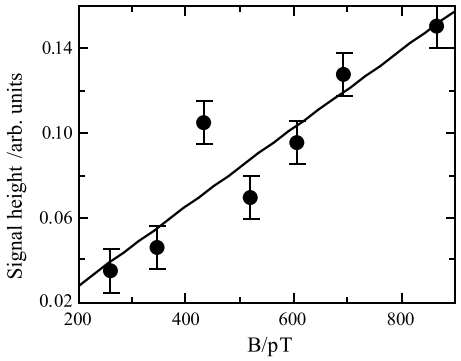

Fig. 3

Fig. 2. – In a longitudinal-magnetic-flux density of 21 μT and with equal circular laser polarizations the coherent population trapping resonance splits into seven Zeeman components. The flux density can be determined with $3 \cdot 10^{-5}$ relative uncertainty from the position of the individual components.

Fig. 3. – Dependence of signal amplitude on the amplitude of a transverse magnetic field modulated at 8 kHz.

Schmidt *et al.* [17], although not specifically with magnetometry in mind. Depending on laser polarizations and magnetic-field direction, up to 15 dark resonances can be observed [18]. In the linear Zeeman regime the shifts of the dark lines are given by $\Delta\nu = 3.5\,\mathrm{Hz/nT}\,(m_3+m_4)\,B$, where m_3 and m_4 are the magnetic quantum numbers of the coupled lower states and B is the magnetic-flux density. Figure 2 shows an example of a dark resonance spectrum for equal circular laser polarizations in a longitudinal magnetic field for a cell with 87 mbar of neon as a buffer gas. The dependence of the relative strengths of all resonances on laser polarizations and magnetic-field direction can be understood with the help of a simple model which gives detailed quantitative agreement with our experimental data both for cells with and without buffer gas [18].

The simplest way to measure magnetic-field strengths is to determine the position of the resonances in a spectrum and use the Breit-Rabi formula for the ground-state energies to extract the flux density from a numerical fit. From spectra like the one in fig. 2 flux densities from 10 μT to 1mT can be determined with typically $3 \cdot 10^{-5}$ relative uncertainty of the numerical fit. For this method the accuracy of the numerical value of B is ultimately limited to about $2 \cdot 10^{-6}$ because from the Breit-Rabi formula one does not obtain B directly but the parameter $x = (g_J - g_I)\mu_\mathrm{B} B/\hbar$, where μ_B is the Bohr magneton and g_J, g_I are the electronic and the nuclear g-factors which are only known to within $1.3 \cdot 10^{-6}$ [19].

The real potential of coherent population trapping for precision magnetometry lies in the detection of small changes of magnetic fields. The general idea is to keep the laser frequency fixed at a value corresponding to the steepest slope of the outermost resonance and detect its Zeeman shift by a change in the absorption or dispersion signal. In order to reduce interference from stray AC and DC magnetic fields these measurements have to be performed in a well-shielded environment. Since no shielding good enough for unperturbed measurements of DC fields in the pT range was available (the noise level at DC corresponds to about 1 nT) a modulation technique was employed in the first experiments. An oscillating magnetic field (instead of frequency modulation of the laser) leads to an oscillating signal which can be demodulated by a narrow-band lock-in amplifier, thus drastically reducing both the influence

of stray fields at different frequencies and of other noise sources such as mechanical vibrations.

An alternating magnetic field $B(t) = B_{\rm const} + B_{\rm mod}\cos(\omega_{\rm mod}t)$ applied to the cesium cell effectively modulates the frequency detuning between the laser field and the dark resonance components via their respective Zeeman shifts. The resulting lineshapes can be explained using a simple model. After averaging over all optical and r.f. frequencies too fast for the photodiode used, the transmitted intensity behind the cesium cell of length l is given by

$$I(\nu, B) = I_0\, e^{-2\delta(\nu,B)}\,, \tag{1}$$

where ν is the relative laser frequency stepped across the resonance and $2\delta(\nu, B)/l$ the absorption coefficient. $I(\nu, B)$ can be replaced by its first-order Taylor expansion around $B_{\rm const}$ for small amplitudes $B_{\rm mod}$. Then lock-in detection yields an in-phase signal

$$S(\nu, B_{\rm const}) = B_{\rm mod}\,\frac{{\rm d}I(B)}{{\rm d}B}\bigg|_{B_{\rm const}}\,. \tag{2}$$

$\delta(\nu, B)$ is given by a superposition of Lorentzian lineshapes for all Zeeman components present. As an example, for a longitudinal field and $\sigma^+\sigma^+$ polarizations δ reads

$$\delta(\nu, B) = \delta_0 \sum_{j=-3}^{j=3} \delta_j \frac{\left(\frac{\Gamma}{2}\right)^2}{(\nu - \nu_0 - 2\,j\,\gamma\,B)^2 + \left(\frac{\Gamma}{2}\right)^2} \tag{3}$$

with $\gamma = 3.5\,{\rm Hz/nT}$ and coefficients $\delta_j = (0.47, 0.68, 0.88, 0.91, 1, 1, 0.75)$ calculated for the experimental configuration of fig. 2 from the theory presented in [18]. Hence the signal becomes

$$S(\nu, B_{\rm const}) \propto B_{\rm mod}\, e^{-2\delta(\nu,B_{\rm const})} \sum_{j=-3}^{j=3} \delta_j \frac{j\,(\nu - \nu_0 - 2\,j\,\gamma\,B_{\rm const})}{(\nu - \nu_0 - 2\,j\,\gamma\,B_{\rm const})^2 + \left(\frac{\Gamma}{2}\right)^2}\,. \tag{4}$$

As seen from this formula the lineshape is asymmetric with respect to the optical frequency ν when $B_{\rm const} \neq 0$. Hence even if this field modulation technique is applied for flux densities below the μT range where different Zeeman lines are not resolved, the DC field can still be determined from the lineshape. Another important point is that for symmetric relative peak strengths $\delta_j = \delta_{-j}$ (as would be the case for high buffer gas pressure [18]) and $B_{\rm const} = 0$ the signal is identically zero.

The total signal strength is expected to be proportional to the amplitude of the alternating field and this was checked in the first experiment. Transverse fields of several hundred pT oscillating at $\nu_{\rm mod} = 8{\rm kHz}$ were applied, generated by a current coil placed at a distance of 1 m from the cell (coated walls but no buffer gas) in order to have a sufficiently homogeneous field. The DC offset field was not compensated completely but a remaining field of several μT split the resonance line into 8 Zeeman components. As expected, the demodulated absorption signal (given by the signal $R = \sqrt{X^2 + Y^2}$ summed over the whole spectrum, where X and Y are the in-phase and quadrature signals of the lock-in amplifier) decreases linearly with the amplitude of the field (fig. 3).

In order to check the sensitivity for fields in the pT range, in a second experiment the cell had to be shielded from external-field fluctuations such as the micropulsations of the geomagnetic field with amplitudes around 1 nT. Therefore the cesium cell was placed inside a two-layer μ-metal cylinder with an estimated longitudinal shielding factor of about 1000. Two wire loops in a Helmholtz configuration provided a longitudinal oscillatory field with a

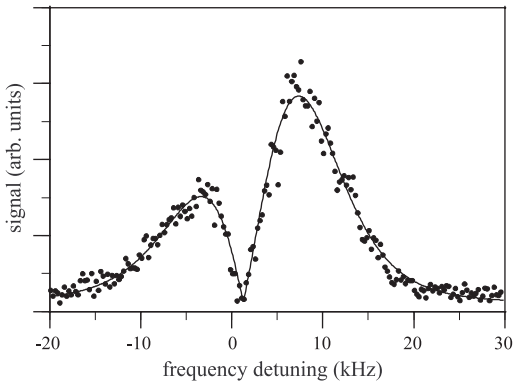

Fig. 4. – Typical field modulation spectrum for 7 pT amplitude and 8 kHz modulation frequency with numerical fit according to eqs. (1)-(4).

calculated flux density of (7.2 ± 0.8) pT. This value is consistent with calibration measurements in the μT range where the flux density was directly determined from the Zeeman splitting of the dark resonance. Figure 4 shows a typical spectrum for 8 kHz modulation frequency with an averaging time of 0.6 s per point together with the theoretical line fit according to the model described above. In this example the constant offset field determined from the fit is (31 ± 3) nT, which is consistent with the strength of the residual geomagnetic field after attenuation by the μ-metal cylinder. We have therefore a modulation method to determine static fields, although only with moderate sensitivity.

From the signal-to-noise ratio S/N and the linear dependence of the signal on the modulation field amplitude one can extrapolate to a minimum detectable change $\Delta B_{\min} = B_{\mathrm{mod}}/(S/N)$. With $S/N \approx 15$ for the case of fig. 4 extrapolated sensitivities below 500 fT (within about a factor of 2) are obtained for modulation frequencies of 5–10 kHz. The noise was taken to be the rms value of the difference between the numerical fit and the experimental values across the resonance.

Of course it is not necessary to always record a whole spectrum in order to determine the AC magnetic flux density. When the signal amplitude at the two maxima of the line shape in fig. 4 is measured, changes in overall amplitude give the change in AC field amplitude, whereas changes in the relative height of the two maxima give information about DC field changes as well as the sign of B.

Since the position of the Zeeman components shifts proportional to $|\vec{B}|$ both types of magnetometer discussed here (figs. 2, 4) are scalar, *i.e.* sensitive to $|\vec{B}|$. However, for suitably chosen laser polarizations the appearance and relative strength of the Zeeman components can also give information about the direction of $\vec{B}$ [18].

In conclusion, we have demonstrated experimental realizations of precision magnetometers based on coherent population trapping. Although they do not yet make use of the particularly advantageous configuration proposed in the theoretical work [8, 9], it is already possible to directly measure longitudinal AC flux densities of a few pT and to extrapolate to below 500 fT from the signal-to-noise ratio, all within 0.5 s integration time per measurement point. With a better magnetic shielding the measurements could be extended to DC fields and noise properties of the dark-state magnetometer could be investigated in detail. It would be interesting to explore whether the record sensitivities of a few fT/$\sqrt{\mathrm{Hz}}$ for an optical pumping magnetometer operating near DC [7] can also be reached with a dark-state magnetometer.

***

This work has been supported in part by the Deutsche Forschungsgemeinschaft and the German Academic Exchange Service (DAAD) through the Vigoni Program.

REFERENCES

[1] Hämäläinen M., Hari R., Ilmoniemi R., Knuutila J. and Lounasmaa O. V., *Rev. Mod. Phys.*, **65** (1993) 413.
[2] Bloom A. L., *Appl. Opt.*, **1** (1962) 61.
[3] Alexandrov E. B. and Bonch-Bruevich V. A., *Optical Engin.*, **31** (1992) 711.
[4] Aleksandrov E. B., Bonch-Bruevich V. A. and Yacobson N. N., *Sov. J. Opt. Technol.*, **60** (1993) 754.
[5] Vodel W. and Mäkiniemi K., *Meas. Sci. Technol.*, **3** (1992) 1155.
[6] Cohen-Tannoudji C., Du Pont-Roc J., Haroche S. and Laloë F., *Phys. Rev. Lett.*, **22** (1969) 758.
[7] Aleksandrov E. B., Balabas M. V., Vershovskii A. K., Ivanov A. E., Yakobson N. N., Velichanskii V. L. and Senkov N. V., *Opt. Spectrosc.*, **78** (1995) 292.
[8] Scully M. O. and Fleischhauer M., *Phys. Rev. Lett.*, **69** (1992) 1360.
[9] Fleischhauer M. and Scully M. O., *Phys. Rev. A*, **49, 3** (1994) 1973.
[10] Alzetta G., Gozzini A., Moi L. and Orriols G., *Nuovo Cimento B*, **36** (1976) 5.
[11] Arimondo E., *Progr. Opt.*, **35** (1996) 257.
[12] Brandt S., Nagel A., Wynands R. and Meschede D., *Phys. Rev. A*, **56** (1997) R1063.
[13] Prevedelli M., Freegarde T. and Hänsch T. W., *Appl. Phys. B*, **60** (1995) 241.
[14] Bjorklund G. C., Levenson M. D., Lenth W. and Ortiz C., *Appl. Phys. B*, **32** (1983) 145.
[15] Akulshin A. M., Celikov A. A. and Velichansky V. L., *Opt. Commun.*, **84** (1991) 139.
[16] Fulton D. J., Moseley R. R., Sheperd S., Sinclair B. D. and Dunn M. H., *Opt. Commun.*, **116** (1995) 231.
[17] Schmidt O., Wynands R., Hussein Z. and Meschede D., *Phys. Rev. A*, **53** (1996) R27.
[18] Wynands R., Nagel A., Brandt S., Meschede D. and Weis A., *Phys. Rev. A.*, **58** (1998) 196.
[19] White C. W., Hughes W. M., Hayne G. S. and Robinson H. G., *Phys. Rev. A*, **7** (1973) 1178.